Geometric tracking control of a quadrotor UAV on SE (3) for extreme maneuverability

Article · January 2010

CITATIONS
68

READS
1,367

3 authors, including:

Melvin Leok
University of California, San Diego
135 PUBLICATIONS **4,580** CITATIONS
SEE PROFILE

N.H. Mcclamroch
University of Michigan
339 PUBLICATIONS **13,268** CITATIONS
SEE PROFILE

Geometric Tracking Control of a Quadrotor UAV on SE(3) for Extreme Maneuverability ⋆

Taeyoung Lee * **Melvin Leok** ** **N. Harris McClamroch** ***

* *Mechanical and Aerospace Engineering, Florida Institute of Technology, Melbourne, FL 39201 (e-mail: taeyoung@fit.edu)*
** *Mathematics, University of California at San Diego, La Jolla, CA 92093 (e-mail: mleok@math.ucsd.edu)*
*** *Aerospace Engineering, University of Michigan, Ann Arbor, MI 48109 (e-mail: nhm@umich.edu)*

Abstract: This paper provides new results for the tracking control of a quadrotor unmanned aerial vehicle (UAV). The dynamics of the quadrotor UAV are expressed globally on the configuration manifold of the special Euclidean group, and we construct geometric controllers to track outputs that correspond to each of three flight modes, namely (1) almost global asymptotic tracking of the attitude of the quadrotor UAV, (2) almost global asymptotic tracking of the position of the center of mass of the quadrotor UAV, and (3) almost global asymptotic tracking of the velocity of the center of mass of the quadrotor UAV. Since the control approach is coordinate-free, it completely avoids singularities and complexities that arise when using local coordinates. Based on a hybrid control architecture, we show that the proposed control system can generate complex acrobatic maneuvers of a quadrotor UAV.

1. INTRODUCTION

A quadrotor unmanned aerial vehicle (UAV) consists of two pairs of counter-rotating rotors and propellers, located at the vertices of a square frame. Due to its simple mechanical structure, it has been envisaged for various applications (see Valenti et al. [2006], Pounds et al. [2010], Hoffmann et al. [2007]).

Despite the substantial interest in quadrotor UAVs, little attention has been paid to constructing nonlinear control systems. Linear control systems are widely used to enhance the stability properties of an equilibrium (see, for example, Valenti et al. [2006], Hoffmann et al. [2007], Castillo et al. [2005], Bouabdalla et al. [2005], Nice [2004]). A nonlinear controller is developed for the linearized dynamics of a quadrotor UAV by Guenard et al. [2005]. Backstepping and sliding mode techniques are applied by Bouabdalla and Siegward [2005]. Since all of these controllers are based on Euler angles, they exhibit singularities when representing complex rotational maneuvers of a quadrotor UAV, thereby significantly restricting their ability to achieve complex flight maneuvers.

Geometric control, as utilized in this paper, is concerned with the development of control systems for dynamic systems evolving on nonlinear manifolds that cannot be globally identified with Euclidean spaces (see Bloch [2003], Bullo and Lewis [2005]). By characterizing geometric properties of nonlinear manifolds intrinsically, geometric control techniques provide unique insights to control theory that cannot be obtained from dynamic models represented using local coordinates. This approach has been applied to fully actuated rigid body dynamics on Lie groups by Bullo and Lewis [2005], Cabecinhas et al. [2008], Chaturvedi et al. [2009].

In this paper, we make use of geometric methods to define and analyze controllers that can achieve complex aerobatic maneuvers for a quadrotor UAV. The dynamics of the quadrotor UAV are expressed globally on the configuration manifold of the special Euclidean group $\mathsf{SE}(3)$. Based on a hybrid control architecture, we construct controllers that can achieve output tracking for outputs that correspond to each of several flight modes. In particular, we introduce three flight modes, each defined by a nonlinear controller that achieves: (1) almost global asymptotic tracking of the attitude of the quadrotor UAV, (2) almost global asymptotic tracking of the position of the center of mass, and (3) almost global asymptotic tracking of the velocity of the center of mass. Since the control approach is coordinate-free, it completely avoids singularities and complexities that arise when using local coordinates. This paper is an extension of the prior work of Lee et al. [2010b], introducing a hybrid control structure, a velocity tracking mode, convergence properties of the first body fixed axis, and a new example. *Due to page limit, all of the proofs are relegated to Lee et al. [2010a].*

2. QUADROTOR DYNAMICS MODEL

Consider a quadrotor UAV model illustrated in Fig. 1. This is a system of four identical rotors and propellers located at the vertices of a square, which generate a thrust and torque normal to the plane of this square. We choose

⋆ This work was supported in part by NSF under grants CMMI-1029551, DMS- 0726263, DMS-1001521, DMS-1010687, and CMMI-1029445.

Preprint submitted to 18th IFAC World Congress. Received October 18, 2010.

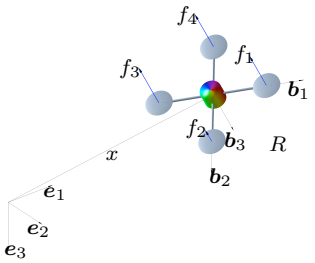

Fig. 1. Quadrotor model

an inertial reference frame $\{\boldsymbol{e}_1, \boldsymbol{e}_2, \boldsymbol{e}_3\}$ and a body-fixed frame $\{\boldsymbol{b}_1, \boldsymbol{b}_2, \boldsymbol{b}_3\}$. The origin of the body-fixed frame is located at the center of mass of this vehicle. The first and the second axes of the body-fixed frame, $\boldsymbol{b}_1, \boldsymbol{b}_2$, lie in the plane defined by the centers of the four rotors. The third body-fixed axis $\boldsymbol{b}_3$ is normal to this plane. Define

$m \in \mathbb{R}$	the total mass
$J \in \mathbb{R}^{3\times 3}$	the inertia matrix with respect to the body-fixed frame
$R \in \mathsf{SO(3)}$	the rotation matrix from the body-fixed frame to the inertial frame
$\Omega \in \mathbb{R}^3$	the angular velocity in the body-fixed frame
$x \in \mathbb{R}^3$	the position vector of the center of mass in the inertial frame
$v \in \mathbb{R}^3$	the velocity vector of the center of mass in the inertial frame
$d \in \mathbb{R}$	the distance from the center of mass to the center of each rotor in the $\boldsymbol{b}_1, \boldsymbol{b}_2$ plane
$f_i \in \mathbb{R}$	the thrust generated by the i-th propeller along the $-\boldsymbol{b}_3$ axis
$\tau_i \in \mathbb{R}$	the torque generated by the i-th propeller about the $\boldsymbol{b}_3$ axis
$f \in \mathbb{R}$	the total thrust, i.e., $f = \sum_{i=1}^4 f_i$
$M \in \mathbb{R}^3$	the total moment vector in the body-fixed frame

The configuration of this quadrotor UAV is defined by the location of the center of mass and the attitude with respect to the inertial frame. Therefore, the configuration manifold is the special Euclidean group $\mathsf{SE(3)}$, which is the semidirect product of $\mathbb{R}^3$ and the special orthogonal group $\mathsf{SO(3)} = \{R \in \mathbb{R}^{3\times 3} \,|\, R^T R = I, \det R = 1\}$.

The following conventions are assumed for the rotors and propellers and the thrust and moment that they exert on the quadrotor UAV. We assume that the thrust of each propeller is directly controlled, i.e., we do not consider the dynamics of rotors and propellers, and the direction of the thrust of each propeller is normal to the quadrotor plane. The first and third propellers are assumed to generate a thrust along the direction $-\boldsymbol{b}_3$ when rotating clockwise; the second and fourth propellers are assumed to generate a thrust along the direction $-\boldsymbol{b}_3$ when rotating counterclockwise. Thus the total thrust magnitude is $f = \sum_{i=1}^4 f_i$ along the direction of $-\boldsymbol{b}_3$. According to the definition of the rotation matrix $R \in \mathsf{SO(3)}$, the total thrust vector is given by $-fRe_3 \in \mathbb{R}^3$ in the inertial frame. We also assume that the torque generated by each propeller is directly proportional to its thrust. Since it is assumed that the first and the third propellers rotate clockwise and the second and the fourth propellers rotate counterclockwise to generate a positive thrust along the direction $-\boldsymbol{b}_3$, the torque generated by the i-th propeller is given by $\tau_i = (-1)^i c_{\tau f} f_i$ for a fixed constant $c_{\tau f}$.

Under these assumptions, the total thrust, and the total moment vector in the body-fixed frame can be written as

$$\begin{bmatrix} f \\ M_1 \\ M_2 \\ M_3 \end{bmatrix} = \begin{bmatrix} 1 & 1 & 1 & 1 \\ 0 & -d & 0 & d \\ d & 0 & -d & 0 \\ -c_{\tau f} & c_{\tau f} & -c_{\tau f} & c_{\tau f} \end{bmatrix} \begin{bmatrix} f_1 \\ f_2 \\ f_3 \\ f_4 \end{bmatrix}. \tag{1}$$

The determinant of the above 4×4 matrix is $8c_{\tau f} d^2$, so it is invertible when $d \neq 0$ and $c_{\tau f} \neq 0$. Therefore, for given total thrust and moment vector f, M, the thrust of each propeller f_1, f_2, f_3, f_4 can be obtained from (1). Using this equation, the total thrust $f \in \mathbb{R}$ and the moment vector $M \in \mathbb{R}^3$ are viewed as control inputs in this paper.

The equations of motion of the quadrotor UAV can be written as

$$\dot{x} = v, \tag{2}$$

$$m\dot{v} = mge_3 - fRe_3, \tag{3}$$

$$\dot{R} = R\hat{\Omega}, \tag{4}$$

$$J\dot{\Omega} + \Omega \times J\Omega = M, \tag{5}$$

where *hat map* $\hat{\cdot} : \mathbb{R}^3 \to \mathfrak{so}(3)$ is defined by the condition that $\hat{x}y = x \times y$ for all $x, y \in \mathbb{R}^3$ (see Appendix A).

3. GEOMETRIC TRACKING CONTROL OF A QUADROTOR UAV

Since the quadrotor UAV has four inputs, it is possible to achieve asymptotic output tracking for at most four quadrotor UAV outputs. This motivates us to introduce several flight modes. Each flight mode is associated with a specified set of outputs for which exact tracking of those outputs define that flight mode.

- Attitude controlled flight mode: the outputs are the attitude of the quadrotor UAV and the controller for this flight mode achieves asymptotic attitude tracking.
- Position controlled flight mode: the outputs are the position vector of the center of mass of the quadrotor UAV and the controller for this flight mode achieves asymptotic position tracking.
- Velocity controlled flight mode: the outputs are the velocity vector of the center of mass of the quadrotor UAV and the controller for this flight mode achieves asymptotic velocity tracking.

A complex flight maneuver can be defined by specifying a concatenation of flight modes together with conditions for switching between them; for each flight mode one also specifies the desired or commanded outputs as time functions. For example, one might define a complex aerobatic flight maneuver for the quadrotor UAV that consists of a hovering flight segment with specified constant position vector, a reorientation segment with specified vehicle attitude, and a surveillance flight segment with specified time-varying position vector. These types of complex aerobatic maneuvers, involving large angle transitions between flight modes, have not been much studied in the literature. Such a hybrid flight control architecture, for longitudinal flight

maneuvers only, has been proposed by Oishi and Tomlin [1999], Ghosh and Tomlin [2000], Oishi and Tomlin [2002].

4. ATTITUDE CONTROLLED FLIGHT MODE

We now introduce a nonlinear controller for the attitude controlled flight mode. We show that this controller achieves almost globally asymptotic attitude tracking, that is the output attitude of the quadrotor UAV asymptotically tracks the commanded attitude.

An arbitrary smooth attitude tracking command $t \to R_d(t) \in \mathsf{SO(3)}$ is given as a function of time. The corresponding angular velocity command is obtained by the attitude kinematics equation as $\hat{\Omega}_d = R_d^T \dot{R}_d$. We first define errors associated with the attitude dynamics of the quadrotor UAV. The attitude and angular velocity tracking error should be carefully chosen as they evolve on the tangent bundle of $\mathsf{SO(3)}$. First, define the real error function on $\mathsf{SO(3)} \times \mathsf{SO(3)}$:

$$\Psi(R, R_d) = \frac{1}{2}\mathrm{tr}\left[I - R_d^T R\right]. \tag{6}$$

This function is locally positive-definite about $R = R_d$ within the region where the rotation angle between R and R_d is less than 180° (see Bullo and Lewis [2005]). For a given R_d, this set can be represented by the sublevel set $L_2 = \{R \in \mathsf{SO(3)} \,|\, \Psi(R, R_d) < 2\}$, which almost covers $\mathsf{SO(3)}$.

The variation of a rotation matrix can be expressed as $\delta R = R\hat{\eta}$ for $\eta \in \mathbb{R}^3$, so that the derivative of the error function is given by

$$\begin{aligned} \mathbf{D}_R \Psi(R, R_d) \cdot R\hat{\eta} &= -\frac{1}{2}\mathrm{tr}\left[R_d^T R \hat{\eta}\right] \\ &= \frac{1}{2}(R_d^T R - R^T R_d)^\vee \cdot \eta, \end{aligned} \tag{7}$$

where the *vee map* $^\vee : \mathfrak{so}(3) \to \mathbb{R}^3$ is the inverse of the hat map. We used a property of the hat map given by equation (A.3) in Appendix A. From this, the attitude tracking error e_R is chosen to be

$$e_R = \frac{1}{2}(R_d^T R - R^T R_d)^\vee. \tag{8}$$

The tangent vectors $\dot{R} \in \mathsf{T}_R\mathsf{SO(3)}$ and $\dot{R}_d \in \mathsf{T}_{R_d}\mathsf{SO(3)}$ cannot be directly compared since they lie in different tangent spaces. We transform $\dot{R}_d$ into a vector in $\mathsf{T}_R\mathsf{SO(3)}$, and we compare it with $\dot{R}$ as follows:

$$\dot{R} - \dot{R}_d(R_d^T R) = R(\Omega - R^T R_d \Omega_d)^\wedge,$$

where $\hat{\Omega}_d = R_d^T \dot{R}_d$ and we use equation (A.5) in Appendix A. This motivates our choice of the tracking error for the angular velocity e_Ω as follows:

$$e_\Omega = \Omega - R^T R_d \Omega_d. \tag{9}$$

We show that e_Ω is the angular velocity of the relative rotation matrix $R_d^T R$, represented in the body-fixed frame, since:

$$\frac{d}{dt}(R_d^T R) = R_d^T R(\Omega - R^T R_d \Omega_d)^\wedge = (R_d^T R)\,\hat{e}_\Omega. \tag{10}$$

We now introduce a nonlinear controller for the attitude controlled flight mode, described by an expression for the total moment:

$$\begin{aligned} M = &-k_R e_R - k_\Omega e_\Omega + \Omega \times J\Omega \\ &- J(\hat{\Omega} R^T R_d \Omega_d - R^T R_d \dot{\Omega}_d), \end{aligned} \tag{11}$$

where k_R, k_Ω are positive constants and $R_d(t) \in \mathsf{SO(3)}$ is the specified attitude command for this attitude controlled flight mode. The control moment vector depends of feedback of the attitude error and angular velocity error and it depends on the commanded attitude, angular velocity and angular acceleration.

In this attitude controlled mode, it is possible to ignore the translational motion of the quadrotor UAV; consequently the reduced model for the attitude dynamics are given by equations (4), (5), using the controller expression (11).

We now show that the reduced closed loop dynamics have the property that $(e_R, e_\Omega) = (0, 0)$ is an equilibrium that is exponentially stable.

Proposition 1. (Exponential Stability of Attitude Controlled Flight Mode) Consider the control moment M defined in (11) for any positive constants k_R, k_Ω. Suppose that the initial conditions satisfy

$$\Psi(R(0), R_d(0)) < 2, \tag{12}$$

$$\|e_\Omega(0)\|^2 < \frac{2}{\lambda_{\max}(J)} k_R (2 - \Psi(R(0), R_d(0))), \tag{13}$$

where $\lambda_{\max}(J)$ denotes the maximum eigenvalue of the inertia matrix J. Then, the zero equilibrium of the closed loop tracking error $(e_R, e_\Omega) = (0, 0)$ is exponentially stable. Furthermore, there exist constants $\alpha_2, \beta_2 > 0$ such that

$$\Psi(R(t), R_d(t)) \le \min\left\{2, \alpha_2 e^{-\beta_2 t}\right\}. \tag{14}$$

In this proposition, equations (12), (13) describe a region of attraction for the reduced closed loop dynamics. An estimate of the domain of attraction is obtained for which the quadrotor attitude lies in the sublevel set $L_2 = \{R \in \mathsf{SO(3)} \,|\, \Psi(R, R_d) < 2\}$. This requires that the initial attitude error should be less than 180°, in terms of the rotation angle about the eigenaxis between R and R_d. Therefore, in Proposition 1, exponential stability is guaranteed for almost all initial attitude errors. The attitude error function defined in (6) has the following critical points or equilibrium solutions: the identity matrix, and rotation matrices that can be written as $\exp(\pi\hat{v})$ for any $v \in \mathsf{S}^2$. These non-identity critical points of the attitude error function lie outside of the region of attraction. Since these critical points are a two-dimensional manifold in the three-dimensional $\mathsf{SO(3)}$, we claim that the presented controller exhibits *almost global* properties in $\mathsf{SO(3)}$. It is impossible to construct a smooth controller on $\mathsf{SO(3)}$ that has global asymptotic stability. The region of attraction for the angular velocity can be increased by choosing a large controller gain k_R in (13).

Asymptotic tracking of the quadrotor attitude does not require specification of the total thrust force. As an auxiliary problem, the total thrust force can be chosen in many different ways to achieve a 1-D translational motion objective. As one illustration of a specific selection approach, we assume that the objective is to asymptotically track a quadrotor altitude command. It is straightfoward to obtain the following corollary of Proposition 1.

Proposition 2. (Exponential Stability of Attitude Controlled Flight Mode with Altitude Tracking) Consider the

control moment M defined in (11) satisfying the assumptions of Proposition 1. In addition, the total thrust force is given by

$$f = \frac{k_x(x_3 - x_{3_d}) + k_v(\dot{x}_3 - \dot{x}_{3_d}) + mg - m\ddot{x}_{3_d}}{e_3 \cdot Re_3}, \quad (15)$$

where k_x, k_v are positive constants, $x_{3d}(t)$ is the quadrotor altitude command, and we assume that

$$e_3 \cdot Re_3 \neq 0. \quad (16)$$

The conclusions of Proposition 1 hold and in addition the quadrotor altitude $x_3(t)$ asymptotically tracks the altitude command $x_{3_d}(t)$.

Since the translational motion of the quadrotor UAV can be only partially controlled; this flight mode is most suitable only for short time periods where an attitude maneuver is to be completed. The translational equations of motion of the quadrotor UAV, during an attitude flight mode, are given by equations (2), (3), and whatever total thrust controller, e.g. equation (15), is selected. These equations can be analyzed to determine the full translational motion of the quadrotor UAV during an attitude controlled flight mode.

5. POSITION CONTROLLED FLIGHT MODE

We now introduce a nonlinear controller for the position controlled flight mode. We show that this controller achieves almost global asymptotic position tracking, that is the output position vector of the quadrotor UAV asymptotically tracks the commanded position. This flight mode requires analysis of the coupled translational and rotational equations of motion; hence, we make use of the notation and analysis in the prior section to describe the properties of the closed loop system in this flight mode.

An arbitrary position tracking command $t \to x_d(t) \in \mathbb{R}^3$ is given. The position tracking errors for the position and the velocity are given by:

$$e_x = x - x_d, \quad (17)$$
$$e_v = v - \dot{x}_d. \quad (18)$$

The nonlinear controller for the position controlled flight mode, described by control expressions for the total thrust magnitude and the total moment vector, are:

$$f = (k_x e_x + k_v e_v + mge_3 - m\ddot{x}_d) \cdot Re_3, \quad (19)$$
$$M = -k_R e_R - k_\Omega e_\Omega + \Omega \times J\Omega - J(\hat{\Omega}R^T R_c \Omega_c - R^T R_c \dot{\Omega}_c), \quad (20)$$

where k_x, k_v, k_R, k_Ω are positive constants. Following the prior definition of the attitude error and the angular velocity error

$$e_R = \frac{1}{2}(R_c^T R - R^T R_c)^\vee, \quad e_\Omega = \Omega - R^T R_c \Omega_c, \quad (21)$$

where $R_c(t) \in \mathsf{SO(3)}$ and $\Omega_c \in R^3$ are constructed as:

$$R_c = [b_{1_c}; b_{3_c} \times b_{1_c}; b_{3_c}], \quad \hat{\Omega}_c = R_c^T \dot{R}_c, \quad (22)$$

where $b_{3_c} \in \mathsf{S}^2$ is defined by

$$b_{3_c} = -\frac{-k_x e_x - k_v e_v - mge_3 + m\ddot{x}_d}{\|-k_x e_x - k_v e_v - mge_3 + m\ddot{x}_d\|}. \quad (23)$$

We usually define position controler as x,y,z = PD, why here its only z?

and $b_{1c} \in \mathsf{S}^2$ is selected to be orthogonal to b_{3c}, thereby guaranteeing that $R_c \in \mathsf{SO(3)}$. We assume that

$$\|-k_x e_x - k_v e_v - mge_3 + m\ddot{x}_d\| \neq 0, \quad (24)$$

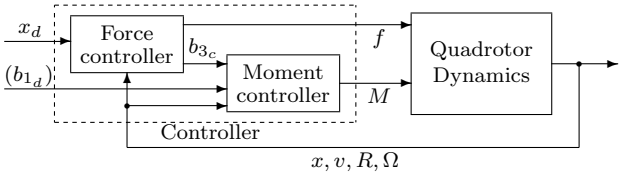

Fig. 2. Controller structure for position controlled flight mode

and

$$\| - mge_3 + m\ddot{x}_d\| < B \quad (25)$$

for a given positive constant B.

The control thrust magnitude and the control moment vector depend on feedback of the position error and translational velocity error and they depend on the commanded position, translational velocity and translational acceleration. The control moment vector has a form that is similar to that for the attitude controlled flight mode. However, the *attitude error* and *angular velocity error* are defined with respect to a computed attitude, angular velocity and angular acceleration, that are constructed according to the indicated procedure. This construction has the property that the direction of the thrust vector, namely $-Re_3$, is such that the thrust magnitude (19) achieves the desired position tracking objectives.

In short, this control system is designed to achieve asymptotic tracking of the complete dynamics. The closed loop system for this position controlled flight mode is illustrated in Fig. 2. The corresponding closed loop control system is described by equations (2), (3), (4), (5), using the controller expressions (19) and (20).

We now show that the closed loop dynamics have the property that $(e_x, e_v, e_R, e_\Omega) = (0, 0, 0, 0)$ is an equilibrium that is exponentially stable.

Proposition 3. (Exponential Stability of Position Controlled Flight Mode) Consider the thrust magnitude f and moment vector M defined in expressions (19), (20). Suppose that the initial conditions satisfy

$$\Psi(R(0), R_c(0)) < 1. \quad (26)$$

Define $W_1, W_{12}, W_2 \in \mathbb{R}^{2\times 2}$ to be

$$W_1 = \begin{bmatrix} \frac{c_1 k_x}{m} & -\frac{c_1 k_v}{2m}(1+\alpha) \\ -\frac{c_1 k_v}{2m}(1+\alpha) & k_v(1-\alpha) - c_1 \end{bmatrix}, \quad (27)$$

$$W_{12} = \begin{bmatrix} k_x e_{v_{\max}} + \frac{c_1}{m} B & 0 \\ B & 0 \end{bmatrix}, \quad (28)$$

$$W_2 = \begin{bmatrix} \frac{c_2 k_R}{\lambda_{\max}(J)} & -\frac{c_2 k_\Omega}{2\lambda_{\min}(J)} \\ -\frac{c_2 k_\Omega}{2\lambda_{\min}(J)} & k_\Omega - c_2 \end{bmatrix}, \quad (29)$$

where $\psi_1 < \Psi(R(0), R_c(0)) < 1$, $\alpha = \sqrt{\psi_1(2-\psi_1)}$, $e_{v_{\max}} = \max\{\|e_v(0)\|, \frac{B}{k_v(1-\alpha)}\}$. For positive constants k_x, k_v, we choose positive constants c_1, c_2, k_R, k_Ω such that

$$c_1 < \min\left\{k_v(1-\alpha),\ \frac{4mk_xk_v(1-\alpha)}{k_v^2(1+\alpha)^2+4mk_x},\ \sqrt{k_xm}\right\}, \tag{30}$$

$$c_2 < \min\left\{k_\Omega,\ \frac{4k_\Omega k_R\lambda_{\min}(J)^2}{k_\Omega^2\lambda_{\max}(J)+4k_R\lambda_{\min}(J)^2},\ \sqrt{k_R\lambda_{\min}(J)}\right\}, \tag{31}$$

$$\lambda_{\min}(W_2) > \frac{4\|W_{12}\|^2}{\lambda_{\min}(W_1)}. \tag{32}$$

Then, the zero equilibrium of the closed loop tracking errors $(e_x, e_v, e_R, e_\Omega) = (0,0,0,0)$ is exponentially stable. A region of attraction is characterized by (26) and

$$\|e_\Omega(0)\|^2 < \frac{2}{\lambda_{\max}(J)}k_R(\psi_1 - \Psi(R(0), R_c(0))). \tag{33}$$

Note that the *attitude error* defined above is based on the computed attitude $R_c \in \mathsf{SO(3)}$, which depends on feedback according to the above specifications. Note that the construction of R_c is not completely determined but involves an orthogonality selection process; this construction freedom arises as a consequence of the fact that R_c is constructed to define the direction of the thrust vector which is invariant for rotations about that direction.

Proposition 3 requires that the initial *attitude error* is less than 90° to achieve exponential stability for this flight mode. Suppose that this is not satisfied, i.e. $1 \leq \Psi(R(0), R_c(0)) < 2$. We can apply the conclusions of Proposition 1 to obtain that the attitude error function Ψ exponentially decreases, and therefore, it enters the region of attraction of Proposition 3 in a finite time. Therefore, by combining the results of Proposition 1 and 3, we can show almost global exponential attractiveness when $\Psi(R(0), R_c(0)) < 2$.

Definition 1. (Exponential Attractiveness Qu [1998]) An equilibrium point $z = 0$ of a dynamic systems is *exponentially attractive* if, for some $\delta > 0$, there exists a constant $\alpha(\delta) > 0$ and $\beta > 0$ such that $\|z(0)\| < \delta$ implies $\|z(t)\| \leq \alpha(\delta)e^{-\beta t}$ for all $t > 0$.

This should be distinguished from the stronger notion of exponential stability, in which the constant $\alpha(\delta)$ in the above bound is replaced by $\alpha(\delta)\|z(0)\|$.

Proposition 4. (Almost Global Exponential Attractiveness of the Position Controlled Flight Mode) Consider the thrust force f and moment vector M defined in expressions (19), (20). Suppose that the initial conditions satisfy

$$1 \leq \Psi(R(0), R_c(0)) < 2, \tag{34}$$

$$\|e_\Omega(0)\|^2 < \frac{2}{\lambda_{\max}(J)}k_R(2 - \Psi(R(0), R_c(0))). \tag{35}$$

Then, the zero equilibrium of the closed loop tracking errors $(e_x, e_v, e_R, e_\Omega) = (0,0,0,0)$ is exponentially attractive.

In Proposition 4, exponential attractiveness is guaranteed for almost all initial attitude errors. Since the critical points of the attitude error function are a two-dimensional manifold in the three-dimensional $\mathsf{SO(3)}$, as discussed in Section 4, we claim that the presented controller exhibits *almost global* properties in $\mathsf{SO(3)}$.

As described above, the construction of the orthogonal matrix R_c involves definition of its third column b_{3_c} by normalization of a feedback function and selection of its first column b_{1_c} to be orthogonal to this third column. The two-dimensional unit vector b_{1_c} can be arbitrarily chosen in the plane normal to b_{3_c}. This reflects the fact that there still remains one degree of freedom in control inputs, since four control inputs of the quadrotor UAV is designed to follow a three-dimensional position command.

The rotation matrix R_c represents the attitude of the quadrotor UAV required to follow a given position command, and according to the structures of the presented position controlled flight mode, the attitude of the quadrotor UAV asymptotically converges to R_c, i.e. $R \to R_c$ as $t \to \infty$. Therefore, by choosing b_{1_c} properly, we can control the direction of the first body fixed axis. However, we cannot control the two-dimensional direction of the first body fixed axis completely arbitrarily, since there exists only one additional degree of freedom in control inputs. More explicitly, there is a constraint that b_{1_c} should lie in the plane normal to b_{3_c} to guarantee $R_c \in \mathsf{SO(3)}$. Here, the additional one dimensional control input is designed to control the *projection* of the first body fixed axis on to the plane normal to b_{3_c}.

There are several ways to specify the desired direction of the first body fixed axis projected on to the plane normal to b_{3_c}. Here, we choose a desired direction $b_{1_d} \in \mathsf{S}^2$, that is not parallel to b_{3_c}, and b_{1_c} is selected to be the projection of b_{1_d} onto the plane normal to b_{3_c}, i.e. $b_{1_c} = \mathrm{Proj}[b_{1_d}]$, where $\mathrm{Proj}[\cdot]$ denotes the normalized projection onto the plane perpendicular to b_{3_c}. In this case, the first body fixed axis does not converge to b_{1_d} exactly, but it converges to the projection of b_{1_d}, i.e. $b_1 \to b_{1_c} = \mathrm{Proj}[b_{1_d}]$ as $t \to \infty$. In other words, the first body fixed axis converges to the intersection of two planes, namely the plane normal to b_{3_c} and the plane spanned by b_{3_c} and b_{1_d} (see Fig. 3). From (23), we observe that b_{3_c} asymptotically converges to the direction of $ge_3 - \ddot{x}_d$. In short, the additional one dimensional input is used to guarantee that the first body fixed axis asymptotically lies in the plane spanned by b_{1_d} and $ge_3 - \ddot{x}_d$.

Suppose that $\ddot{x}_d = 0$, then the third body fixed axis converges to the gravity direction e_3. In this case, we can choose b_{1_d} arbitrarily in the horizontal plane, which follows that $b_{1_c} = \mathrm{Proj}[b_{1_d}] = b_{1_d}$ as $t \to \infty$. Therefore, the first body fixed axis b_1 asymptotically converges to b_{1_d}, which can be used to specify the heading direction of the quadrotor UAV in the horizontal plane. These are summarized as follows.

Proposition 5. (Almost Global Exponential Attractiveness of Position Controlled Flight Mode with Asymptotic Direction of First Body-Fixed Axis) Consider the moment vector M defined in (20) and the total thrust f defined in (19) satisfying the assumptions of Propositions 3 and 4.

In addition, the first column of R_c, namely b_{1_c} is constructed as follows. We choose $t \to b_{1_d}(t) \in \mathsf{S}^2$, and we assume that it is not parallel to b_{3_c}. The unit vector $\boldsymbol{b}_{1_c}$ is constructed by projecting b_{1_d} onto the plane normal to b_{3_c}:

$$b_{1_c} = \mathrm{Proj}[b_{1_d}] = -\frac{1}{\|b_{3_c} \times b_{1_d}\|}(b_{3_c} \times (b_{3_c} \times b_{1_d})). \tag{36}$$

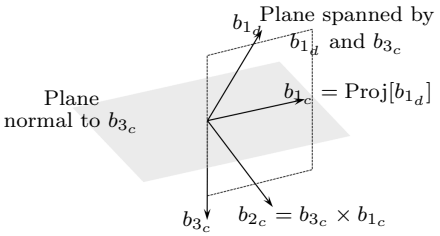

Fig. 3. Convergence property of the first body fixed axis: b_{3_c} is determined by (23). Then, there still remains one additional input degree of freedom, that corresponds to the direction of b_{1_c} in the plane normal to b_{3_c}. We choose an arbitrary b_{1_d} that is not parallel to b_{3_c}, and project it on to the plane normal to b_{3_c} to obtain b_{1_c}. This guarantees that the first body fixed axis asymptotically lies in the plane spanned by b_{1_d} and b_{3_c}, which converges to the direction of $ge_3 - \ddot{x}_d$ as $t \to \infty$.

Then, the conclusions of Propositions 3 and 4 hold, and the first body fixed axis asymptotically lies in the plane composed of b_{1_d} and $ge_3 - \ddot{x}_d$.

In a special case when $\ddot{x}_d = 0$. We choose b_{1_d} on the horizontal plane. Then, the first body fixed axis asymptotically converges to b_{1_d}.

These additional properties of the closed loop can be interpreted as characterizing the asymptotic direction of the first body-fixed axis and the asymptotic direction of the third body-fixed axis as it depends on the commanded vehicle acceleration. These physical properties may be of importance in some flight maneuvers.

The control input of the position controlled flight mode depends on Ω_c and $\dot{\Omega}_c$ as shown at (20). The expressions for Ω_c and $\dot{\Omega}_c$ corresponding to Proposition 5 are summarized at Appendix.

6. VELOCITY CONTROLLED FLIGHT MODE

We now introduce a nonlinear controller for the velocity controlled flight mode. We show that this controller achieves almost global asymptotic velocity tracking, that is the output velocity vector of the quadrotor UAV asymptotically tracks the commanded velocity.

An arbitrary velocity tracking command $t \to v_d(t) \in \mathbb{R}^3$ is given. The velocity tracking error given by:

$$e_v = v - v_d. \tag{37}$$

The nonlinear controller for the velocity controlled flight mode, described by control expressions for the total thrust magnitude and the total moment vector, are:

$$f = (k_v e_v + mge_3 - m\dot{v}_d) \cdot Re_3, \tag{38}$$

$$M = -k_R e_R - k_\Omega e_\Omega + \Omega \times J\Omega - J(\hat{\Omega} R^T R_c \Omega_c - R^T R_c \dot{\Omega}_c), \tag{39}$$

where k_v, k_R, k_Ω are positive constants, and following the prior definition of the attitude error and the angular velocity error

$$e_R = \frac{1}{2}(R_c^T R - R^T R_c)^\vee, \quad e_\Omega = \Omega - R^T R_c \Omega_c, \tag{40}$$

and $R_c(t) \in \mathsf{SO(3)}$ and $\Omega_c \in R^3$ are constructed as:

$$R_c = [b_{1_c}; b_{3_c} \times b_{1_c}; b_{3_c}], \quad \hat{\Omega}_c = R_c^T \dot{R}_c, \tag{41}$$

where $b_{3_c} \in \mathsf{S}^2$ is defined by

$$b_{3_c} = -\frac{-k_v e_v - mge_3 + m\dot{v}_d}{\|-k_v e_v - mge_3 + m\dot{v}_d\|}. \tag{42}$$

and $b_{1c} \in \mathsf{S}^2$ is selected to be orthogonal to b_{3c}, thereby guaranteeing that $R_c \in \mathsf{SO(3)}$. We assume that

$$\|-k_v e_v - mge_3 + m\ddot{x}_d\| \neq 0, \tag{43}$$

and

$$\| - mge_3 + m\ddot{x}_d\| < B \tag{44}$$

for a given positive constant B.

The overall controller structure is similar to the position controlled flight mode. The control thrust magnitude and the control moment vector depend on feedback of the translational velocity error and they depend on the commanded translational velocity and translational acceleration. The control moment vector has a form that is similar to that for the attitude controlled flight mode. However, the *attitude error* and *angular velocity error* are defined with respect to a computed attitude, angular velocity and angular acceleration, that are constructed according to the indicated procedure. This construction has the property that the direction of the thrust vector, namely $-Re_3$, is such that the thrust magnitude (19) achieves the desired velocity tracking objectives. This is again verified in the proof.

We now show that the closed loop dynamics have the property that $(e_v, e_R, e_\Omega) = (0, 0, 0)$ is an equilibrium that is exponentially stable.

Proposition 6. (Exponential Stability of Velocity Controlled Flight Mode) Consider the thrust magnitude f and moment vector M defined in expressions (38), (39). Suppose that the initial conditions satisfy

$$\Psi(R(0), R_c(0)) < 1. \tag{45}$$

Define $W_2 \in \mathbb{R}^{2\times 2}$ to be

$$W_2 = \begin{bmatrix} \frac{c_2 k_R}{\lambda_{\max}(J)} & -\frac{c_2 k_\Omega}{2\lambda_{\min}(J)} \\ -\frac{c_2 k_\Omega}{2\lambda_{\min}(J)} & k_\Omega - c_2 \end{bmatrix}, \tag{46}$$

For positive constants k_v, we choose positive constants c_2, k_R, k_Ω such that

$$c_2 < \min\left\{k_\Omega, \frac{4k_\Omega k_R \lambda_{\min}(J)^2}{k_\Omega^2 \lambda_{\max}(J) + 4k_R \lambda_{\min}(J)^2}, \sqrt{k_R \lambda_{\min}(J)}\right\}, \tag{47}$$

$$\lambda_{\min}(W_2) > \frac{4B^2}{k_v(1-\alpha)}, \tag{48}$$

where $\psi_1 < \Psi(R(0), R_c(0)) < 1$, $\alpha = \sqrt{\psi_1(2-\psi_1)}$. Then, the zero equilibrium of the closed loop tracking errors $(e_v, e_R, e_\Omega) = (0, 0, 0)$ is exponentially stable. A region of attraction is characterized by (45) and

$$\|e_\Omega(0)\|^2 < \frac{2}{\lambda_{\max}(J)} k_R(\psi_1 - \Psi(R(0), R_c(0))). \tag{49}$$

Proposition 6 requires that the initial attitude error is less than 90° to achieve exponential stability for this flight mode. Similar to Proposition 4, we can show almost global exponential attractiveness when $\Psi(R(0), R_c(0)) < 2$.

Proposition 7. (Almost Global Exponential Attractiveness of Velocity Controlled Flight Mode) Consider the thrust force f and moment vector M defined in expressions (38), (39). Suppose that the initial conditions satisfy

$$1 \leq \Psi(R(0), R_c(0)) < 2, \tag{50}$$

$$\|e_\Omega(0)\|^2 < \frac{2}{\lambda_{\max}(J)} k_R (2 - \Psi(R(0), R_c(0))). \tag{51}$$

Then, the zero equilibrium of the closed loop tracking errors $(e_v, e_R, e_\Omega) = (0, 0, 0)$ is exponentially attractive.

As described in Section 5, there is one-dimensional freedom in constructing $R_c \in \mathsf{SO(3)}$, namely the direction of the quadrotor UAV in the plane normal to b_{3_c}. This can be chosen as discussed in Proposition 5.

Proposition 8. (Almost Global Exponential Attractiveness of Velocity Controlled Flight Mode with Asymptotic Direction of First Body-Fixed Axis) Consider the moment vector M defined in (39) and the total thrust f defined in (38) satisfying the assumptions of Propositions 6 and 7.

In addition, the first column of R_c, namely b_{1_c} is constructed as follows. We choose $t \to b_{1_d}(t) \in \mathsf{S}^2$, and we assume that it is not parallel to b_{3_c}. The unit vector $\boldsymbol{b}_{1_c}$ is constructed by projecting b_{1_d} onto the plane normal to b_{3_c}:

$$b_{1_c} = -\frac{1}{\|b_{3_c} \times b_{1_d}\|}(b_{3_c} \times (b_{3_c} \times b_{1_d})). \tag{52}$$

Then, the conclusions of Propositions 6 and 7 hold, and the first body fixed axis asymptotically lies in the plane composed of b_{1_d} and $ge_3 - \dot{v}_d$.

In a special case when $\dot{v}_d = 0$. We choose b_{1_d} on the horizontal plane. Then, the first body fixed axis asymptotically converges to b_{1_d}.

7. NUMERICAL EXAMPLE

Numerical results are presented to illustrate the prior approach to determining complex flight maneuvers for a typical quadrotor UAV. The parameters of the quadrotor UAV are chosen according to a quadrotor UAV developed in Pounds et al. [2010].

$$J = [0.0820, 0.0845, 0.1377]\,\mathrm{kg-m^2}, \quad m = 4.34\,\mathrm{kg}$$

$$d = 0.315\,\mathrm{m}, \quad c_{\tau f} = 8.004 \times 10^{-3}\,\mathrm{m}.$$

The controller parameters are chosen as follows:

$$k_x = 16m, \quad k_v = 5.6m, \quad k_R = 8.81, \quad k_\Omega = 2.54.$$

We consider a complex flight maneuver involving transitions between five flight modes (see Fig. 4). The tracking command for each flight mode is given by

(a) Velocity controlled flight mode ($t \in [0, 4)$)
$v_d(t) = [1 + 0.5t,\ 0.2\sin(2\pi t),\ -0.1], \quad b_{1_d}(t) = [1, 0, 0].$

(b) Attitude controlled flight mode ($t \in [4, 6)$): rotation about $\boldsymbol{e_2}$ by 720°
$$R_d(t) = \exp(2\pi(t-4)\hat{e}_2).$$

(c) Position controlled flight mode ($t \in [6, 8)$)
$$x_d(t) = [14 - t,\ 0,\ 0], \quad b_{1_d}(t) = [1, 0, 0].$$

(d) Attitude controlled flight mode ($t \in [8, 9)$): rotation about $\boldsymbol{e}_1$ by 360°
$$R_d(t) = \exp(2\pi(t-8)\hat{e}_1).$$

(e) Position controlled flight mode ($t \in [9, 12]$)
$$x_d(t) = [20 - \frac{5}{3}t,\ 0,\ 0], \quad b_{1_d}(t) = [0, 1, 0].$$

$$x(0) = [0, 0, 0], \quad v(0) = [0, 0, 0],$$
$$R(0) = I, \quad \Omega(0) = [0, 0, 0].$$

Simulation results for these three flight maneuvers are illustrated at Figure 5. It begins with a velocity controlled flight mode. As the initial attitude error function is less than 1, according to Proposition 6, the velocity tracking error exponentially converges as shown at Fig. 5(d). From Proposition 8, the first body fixed axis asymptotically lies in the plane spanned by b_{1_d} and $ge_3 - \dot{v}_d$. Since $\|\dot{v}_d\| < g$, it stays close to the plane composed of e_1 and e_3, as illustrated at Fig. 5(e).

This is followed by an attitude tracking mode to rotate the quadrotor by 720° about $\boldsymbol{e}_2$. During this time period, the attitude error converges according to Proposition 1, but the quadrotor altitude decreases by 1 meter. But, a position tracking mode is again engaged, and the quadrotor UAV soon follows a straight line again. Another attitude tracking mode and a position tracking mode are repeated to rotate the quadrotor by 360° about the direction of the velocity vector. For the position tracking modes (c) and (e), we have $\ddot{x}_d = 0$, and b_{1_d} lies in the horizontal plane. Therefore, according to Proposition 5, the first body fixed b_1 asymptotically converges to b_{1_d}, as shown at Fig. 5(e). For example, at the last position tracking mode (e), the first body fixed axis points the left side of the flight path since b_{1_d} is specified to be e_2. These illustrate that by switching between an attitude mode and a position and heading flight mode, the quadrotor UAV can perform the indicated complex acrobatic maneuver.

Switching controllers/ references

Appendix A. PROPERTIES OF THE *HAT* MAP

The hat map $\hat{\cdot} : \mathbb{R}^3 \to \mathfrak{so}(3)$ is defined such that $\hat{x}y = x \times y$ for any $x, y \in \mathbb{R}^3$. This identifies the Lie algebra $\mathfrak{so}(3)$ with $\mathbb{R}^3$ using the vector cross product in $\mathbb{R}^3$. The inverse of the hat map is referred to as the *vee* map, $\vee : \mathfrak{so}(3) \to \mathbb{R}^3$. Several properties are summarized as follows.

$$\hat{x}y = x \times y = -y \times x = -\hat{y}x, \tag{A.1}$$

$$-\frac{1}{2}\mathrm{tr}[\hat{x}\hat{y}] = x^T y, \tag{A.2}$$

$$= \mathrm{tr}[A\hat{x}] = \frac{1}{2}\mathrm{tr}[\hat{x}(A - A^T)] = -x^T(A - A^T)^\vee, \tag{A.3}$$

$$\hat{x}A + A^T\hat{x} = (\{\mathrm{tr}[A]\, I_{3\times 3} - A\}\, x)^\wedge, \tag{A.4}$$

$$R\hat{x}R^T = (Rx)^\wedge, \tag{A.5}$$

for any $x, y \in \mathbb{R}^3$, $A \in \mathbb{R}^{3\times 3}$, and $R \in \mathsf{SO(3)}$.

REFERENCES

A. M. Bloch. *Nonholonomic Mechanics and Control*, volume 24 of *Interdisciplinary Applied Mathematics*. Springer-Verlag, 2003.

S. Bouabdalla and R. Siegward. Backstepping and sliding-mode techniques applied to an indoor micro quadrotor. In *Proceedings of the IEEE International Conference on Robotics and Automation*, pages 2259–2264, 2005.

S. Bouabdalla, P. Murrieri, and R. Siegward. Towards autonomous indoor micro VTOL. *Autonomous Robots*, 18(2):171–183, 2005.

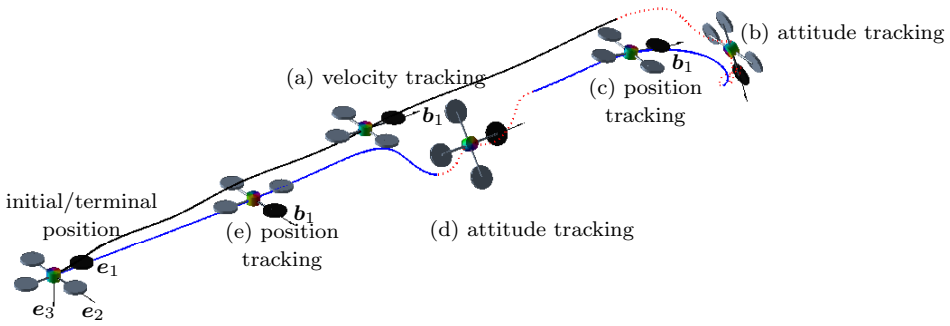

Fig. 4. Complex maneuver of a quadrotor UAV involving a rotation by 720° about e_2 (b), and a rotation by 360° about e_1 (d), with transitions between several flight modes (an animation illustrating this maneuver is available at http://my.fit.edu/~taeyoung).

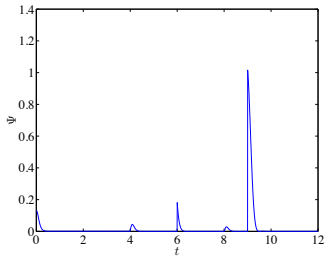

(a) Attitude error function Ψ

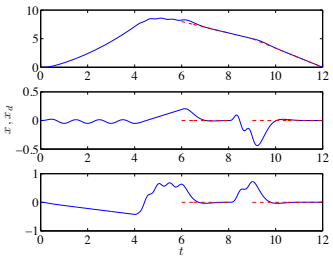

(b) Position (x:solid, x_d:dotted, (m))

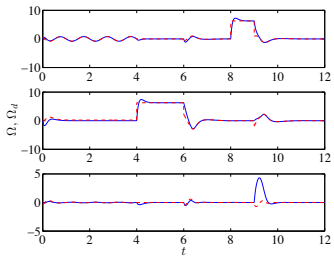

(c) Angular velocity (Ω:solid, Ω_d:dotted, (rad/sec))

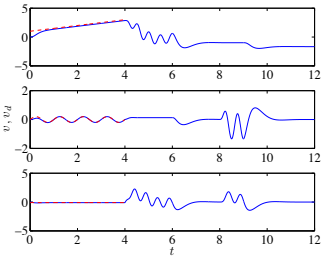

(d) Velocity (v:solid, v_d:dotted, (m/s))

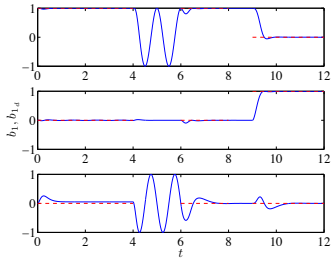

(e) First body fixed axis (b_1:solid, b_{1_d}:dotted)

Fig. 5. Simulation results

F. Bullo and A. D. Lewis. *Geometric control of mechanical systems*, volume 49 of *Texts in Applied Mathematics*. Springer-Verlag, New York, 2005. Modeling, analysis, and design for simple mechanical control systems.

D. Cabecinhas, R. Cunha, and C. Silvestre. Output-feedback control for almost global stabilization of fully-acuated rigid bodies. In 3583-3588, editor, *Proceedings of IEEE Conference on Decision and Control*, 2008.

P. Castillo, R. Lozano, and A. Dzul. Stabilization of a mini rotorcraft with four rotors. *IEEE Control System Magazine*, pages 45–55, 2005.

N. A. Chaturvedi, N. H. McClamroch, and D. Bernstein. Asymptotic smooth stabilization of the inverted 3-D pendulum. *IEEE Transactions on Automatic Control*, 54(6):1204–1215, 2009.

R. Ghosh and C. Tomlin. Nonlinear inverse dynamic control for mode-based flight. In *Proceedings of the AIAA Guidance, Navigation and Control Conference*, 2000.

N. Guenard, T. Hamel, and V. Moreau. Dynamic modeling and intuitive control strategy for an X4-flyer. In *Proceedings of the IEEE International Conference on Control and Application*, 2005.

G. Hoffmann, H. Huang, S. Waslander, and C. Tomlin. Quadrotor helicopter flight dynamics and control: Theory and experiment. In *Proceedings of the AIAA Guidance, Navigation, and Control Conference*, 2007. AIAA 2007-6461.

T. Lee, M. Leok, and N. H. McClamroch. Geometric tracking control of a quadrotor UAV on SE(3). arXiv:1003.2005v1, 2010a. URL `http://arxiv.org/abs/1003.2005v1`.

T. Lee, M. Leok, and N. H. McClamroch. Geometric tracking control of a quadrotor UAV on SE(3). In *Proceedings of the IEEE Conference on Decision and Control*, 2010b. accepted.

E. Nice. Design of a four rotor hovering vehicle. Master's thesis, Cornell University, 2004.

M. Oishi and C. Tomlin. Switched nonlinear control of a vstol aircraft. In *Proceedings of IEEE Conference on Decision and Control*, pages 2685–2690, 1999.

M. Oishi and C. Tomlin. Switching in nonlinear minimum phase systems: Applications to a vstol aircraft. In *Proceedings of American Control Conference*, 2002.

P. Pounds, R. Mahony, and P. Corke. Modeling and control of a large quadrotor robot. *Control Engineering Practice*, 18:691–699, 2010.

Zhihua Qu. *Robust Control of Nonlinear Uncertain Systems*. John Wiley & Sons, Inc., New York, NY, USA, 1998. ISBN 0471115894.

M Valenti, B. Bethke, G. Fiore, and J. How. Indoor multi-vehicle flight testbed for fault detection, indoor multi-vehicle flight testbed for fault detection, isolation, and recovery. In *Proceedings of the AIAA Guidance, Navigation and Control Conference*, 2006.